Physica A 515 (2019) 47–56

Contents lists available at ScienceDirect

Physica A

journal homepage: www.elsevier.com/locate/physa

An extended cost potential field cellular automaton model for pedestrian evacuation considering the restriction of visual field

Xingli Li [a], Fang Guo [a], Hua Kuang [b,*], Zhongfei Geng [a], Yanhong Fan [a]

[a] School of Applied Science, Taiyuan University of Science and Technology, Taiyuan, 030024, China
[b] College of Physical Science and Technology, Guangxi Normal University, Guilin 541004, China

HIGHLIGHTS

- An extended cost potential CA model describing the restriction of visual field is presented.
- A visibility function is introduced to describe visual effect.
- The extended cost function is related to three factors: density, behavior variation and visual effect.
- Evacuation time relies on visual radius and initial density.
- A moderate tension degree can improve the evacuation efficiency at low density.

ARTICLE INFO

Article history:
Received 5 May 2018
Received in revised form 4 September 2018
Available online 27 September 2018

Keywords:
Pedestrian evacuation
Visibility function
Cost potential field
Psychological tension
Cellular automaton model

ABSTRACT

Pedestrian dynamics with affected visual field under emergency situation is a difficult point in the simulation of pedestrian flow. In this paper, an extended cost potential field cellular automaton model is proposed to investigate the motion of pedestrians through obscure room lack of visibility (due to smoke, darkness, etc.). A novel visibility function is introduced to describe visual effect caused by poor vision, which will lead to the increasing cost of discomfort. The numerical simulations are performed to explore the effects of factors, such as psychology tension, visual radius and pedestrian density on pedestrian evacuation. It was found that evacuation time relies on visual radius and initial density. The evacuation time under affected visual field increases with the decrease of visual radius. At low density, a moderate tension degree can improve the evacuation efficiency. These findings will be helpful in pedestrian control and management under an emergency.

1. Introduction

Pedestrian dynamics is the basis of the management of pedestrian evacuations and the design of pedestrian facilities, which contributes to the reasonable design of walking facilities and evacuation rules. Understanding pedestrian flow characteristics beforehand is extremely important in emergency management to improve evacuation procedures and relevant regulations [1,2]. The dynamic properties of pedestrian crowds, including various self-organization phenomena, have been observed and successfully reproduced by various physical methods. Generally, pedestrian flow models can be mainly classified into two categories: macroscopic [3–8] and microscopic [9–31]. Microscopic models include social force model [9–13], lattice gas model [14–19] and cellular automata model [20–30]. Because the concept of cellular automata

* Corresponding author.
E-mail address: khphy@gxnu.edu.cn (H. Kuang).

https://doi.org/10.1016/j.physa.2018.09.145
0378-4371/

model is simple and it is easy to simulate in computer, based on the characteristics of individual pedestrian and system surroundings, the original CA models are combined, extended, or improved to approximate pedestrian dynamics, especially in the evacuation from a room [23–28].

In most simulations of pedestrian evacuation related to the above research, the room is supposed to be under favorable sight conditions. However, the visible scope of pedestrians is often affected by fire/smog, electricity outage, panicked mood, etc. Under the condition with adverse sight, due to a decrease in sight scope, pedestrians show movement behaviors different from those with favorable sight. These behaviors are critical in reflecting the characteristics of the pedestrian evacuation process under adverse sight conditions. However, evacuation exercise under adverse sight may be difficult than normal pedestrian flow because of the danger and possible crowd disaster caused by incidents. To explore macroscopic feature and jamming formation mechanism without visibility, various modeling approaches to study evacuation behavior have been proposed.

Mantovani et al. investigated the effect of red and green indicator on the virtual library scene under poor visibility [32]. Nagai et al. simulated the movement of students with multiple exits and discussed the evacuation process in the dark room [33]. Nagatani et al. modeled the pedestrian evacuation process in a single exit dark room with considering the biased random walk of pedestrian [34]. Yuan et al. studied the effect of smoke on pedestrian evacuation [35]. Emilio et al. studied the motion of pedestrians through obscure corridors where the lack of visibility hides the precise position of the exits [36]. Frank et al. modeled the effects of low visibility by considering three pedestrians behavioral patterns (i.e., individualistic, herding-like and the "following the wall") during the evacuation of pedestrian from a single exit room [37]. Song et al. investigated the effect of visible domain for evacuation signs on the pedestrian flow and found that how to set evacuation signs has a significant effect on the evacuation [38]. Cao et al. proposed a multi-grid evacuation model without visibility through evacuation characteristics of the blind [39].

In 2012, Zhang et al. established a cellular automata model of pedestrian flow that defines a cost potential field, which takes into account the costs of travel time and discomfort in the journey, for a pedestrian to move to an empty neighboring cell [40]. Without the discomfort term, the resulting cost potential in a cell would simply measure the distance between the cell and the destination, which is independent of time and similar to the static field in the floor field CA model (see Ref. [20]). With the discomfort term, the cost distribution increases with the local density, which is reconstructed at each time step and, thus, is time dependent. In this case, the resulting cost potential field is similar to the dynamic field in the floor field CA model. In 2014, Jian et al. proposed a perceived potential field cellular automata model with an aggregated force field to simulate the pedestrian evacuation in a walking domain with poor visibility or complex geometries [41]. Recently, the authors have extended this model to simulate the behavior variation of pedestrian flow from nervous emotion in a room and counter flow, respectively [42,43]. In real life, the lack of understanding the information surrounding the room for the pedestrians can influence the selection of movement, which will inevitably cause the increase of discomfort.

Compared with the previous studies about pedestrian flow under adverse conditions, the different psychological tensions and the induced corresponding behavior variations under emergency have not been perfectly considered up to now. This is insufficient to describe a more general pedestrian flow, where pedestrians might have been influenced by the internal behavior variations due to psychological tension and the external environment. How do these factors affect the pedestrian dynamics in the evacuation? This is an interesting but still open problem. Motivated by the above reasons, in this paper, we use an extended cost potential field CA model combined with abnormal nervousness to simulate pedestrian flow under poor vision. This model enables analysis of the effect of different level of tension, visibility radius and pedestrian density on pedestrian movement under an absence of visual field. The paper is organized as follows. Section 2 describes the new cost potential field CA model integrated with a visibility functions. Section 3 gives simulation results and corresponding discussion, followed by conclusions in the final section.

2. Model

We consider a room divided into $L \times L$ finite two-dimensional grids. The black border denotes the room wall. Each of the other grids can be empty or occupied by a pedestrian and is equivalent to a cell whose size can be approximately regarded as $0.4 \times 0.4\ \mathrm{m}^2$, where L and W are the width of the room and the exit, respectively. As shown in Fig. 1, the whole system is divided into two regions: region A indicates exit-visible area and region B represents exit-invisible area. The sets Ω, Ω_1 and Ω_2 are used to represent the whole system area, region A and region B, respectively. The semicircle near the exit represents that the exit position can be seen and its radius is set R. Exit logo is the exit position and is represented by set Γ. The solid circle denotes the pedestrian. Here it is assumed that the visual radius of each pedestrian is equal and its size is R, e.g., a red solid circle denotes a pedestrian located in the center whose visual radius is R (see Fig. 1).

2.1. Quantitative description of behavior variation

As we know, human psychological characteristics under the emergency situation will inevitably lead to the "rational" or "irrational" behavior. Here the parameter $\eta(0 \leq \eta \leq 1)$ is introduced to describe the influence of nervousness μ on behavior variation and it is defined as follows [42]:

$$\eta(t) = \begin{cases} 0 & 0 \leq \mu \leq 0.05 \\ k_1\mu + a_1 & 0.05 < \mu \leq 0.6 \\ \exp(k_2\mu) + a_2 & 0.6 < \mu \leq 1 \end{cases} \tag{1}$$

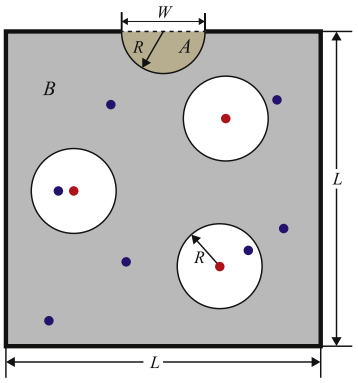

Fig. 1. The illustration of different areas.

where μ represents the level of tension of pedestrian under emergency, and it can be quantitatively described as $\mu(t) = \frac{v_0(t)-v_0(0)}{v_{\max}(t)-v_0(0)}$. Eq. (1) shows that the behavior variation caused by the level of tension can be neglected when the level of tension is very small ($\mu \leq 0.05$), which means pedestrians are in a rational state. When the level of tension is $0.05 < \mu \leq 0.6$, it will lead to a linear increase of the behavior variation. However, when the level of tension increases to $\mu > 0.6$, namely, the level of tension exceeds the critical value of psychological endurance, the behavior variation will have an exponential growth since a person with an extreme panic becomes so frightened and confused. We set the same parameters (see Ref. [43]) in Eq. (1) as $k_1 = 0.247$, $k_2 = 0.98$, $a_1 = -0.012$, $a_2 = -1.66$.

2.2. The cost potential field considering behavior variation

The cost potential is defined by Zhang et al. as the minimal cost for traveling from one cell to the destination [40]. Here, a cost potential function including two terms is introduced: one is the cost of traveling time determined by the pedestrian's walking speed and the distance from the present position to the target position, the other is the cost of discomfort depending on the surrounding density. Based on this study, the authors extended the cost potential field cellular automaton to study pedestrian evacuation in a room and found that behavior variation under an emergency can affect the cost of discomfort and may improve evacuation efficiency [43], define the cost distribution $\tau(x, y, t)$ in a cell (x, y) as

$$\tau(x, y, t) = \frac{1}{v_{\max}} + g(\rho) + h(\eta) \tag{2}$$

where $g(\rho)$ represents the discomfort of pedestrians related to density, $h(\eta)$ denotes the discomfort of pedestrians caused by the behavior variation due to nervousness.

The total cost of walking from cell (x, y) to (x_0, y_0) is

$$\phi(x, y, t) = \int_{(x,y)}^{(x_0,y_0)} (\tau(x, y, t)x'(s)\mathrm{d}x + \tau(x, y, t)y'(s)\mathrm{d}y) \tag{3}$$

We assume that the integral is independent of the path, i.e.,

$$\phi_x(x, y, t) = -\tau(x, y, t)x'(s)\ ,\ \ \phi_y(x, y, t) = -\tau(x, y, t)y'(s)$$

2.3. The cost potential field CA model considering visibility effect

Compared with the good vision environment, the visibility level will affect the pedestrians' discomfort in the process of movement. Here, we introduce a new visibility function w to describe the visibility effect under emergency. Generally speaking, this function is related with such factors as the familiarity with the surrounding environment, the position of exit, the visual ability and the influence of pedestrians around. In this paper, we assume the visibility function w is mainly influenced by the visual radius R and the pedestrians around in the visual radius R.

(1) The ability for the pedestrian to identify the environment depends on the visual radius of the pedestrian in the evacuation system. The visual area of pedestrian is specified as a circle with a radius R, and using the set Ω_3 to represent this area. The smaller the visual radius R, the weaker the ability for pedestrian to identify the surrounding environment. The system is divided into two parts by comparing the distance l_{xy} between the center pedestrian and the exit location set Γ: exit-visible area ($l_{xy} \leq R$) and exit-invisible area ($l_{xy} > R$).

(2) The influence of other pedestrians in the visual area on central pedestrian is used to reflect the impact of blind conformity on visibility function. As shown in Fig. 2, the red arrow and green arrow represent the desired direction for central cell (x, y) and actual direction for the other cell (x_1, y_1), respectively. Here, it is assumed that the angle between the

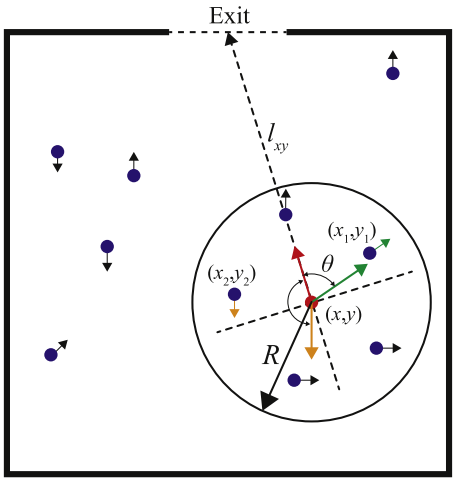

Fig. 2. The influence of the moving direction for surrounding pedestrian on the desired moving direction for the center pedestrian. (For interpretation of the references to color in this figure legend, the reader is referred to the web version of this article.)

desired direction and actual direction is θ, its influence can be quantitatively described as $S_{x_1y_1} = v_{x_1y_1} \cdot \cos\theta$. If $\theta < \frac{\pi}{2}$, the angle between the desired direction and actual direction is an acute angle, which will attract the central pedestrian; if $\theta > \frac{\pi}{2}$, the corresponding angle is an obtuse angle, which means that the desired direction of central pedestrian is repelled by surrounding pedestrians; if $\theta = \frac{\pi}{2}$, the desired direction and actual direction are perpendicular to each other, which means that the interaction force is treated as zero. Therefore, it is assumed that the total number of pedestrians in the visual area is n, the effect by pedestrians around can be quantitatively described as:

$$S_{xy} = \sum_{(x_i,y_i)\in\Omega_3}^{n} S_{x_iy_i} \tag{4}$$

Within the visual field of Ω_3, $S_{xy} > 0$ reflects the attractive force of other pedestrians on the central pedestrian' moving direction; $S_{xy} < 0$ represents the repulsive force of other pedestrians on the central pedestrian' moving direction; $S_{xy} = 0$ indicates that the central pedestrian will not be affected by external forces. From the above mentioned, the attractive force is $S^1_{xy} = \sum^n_{(x_i,y_i)\in\Omega_3} S_{x_iy_i}$ and the repulsive force is $S^2_{xy} \sum^n_{(x_i,y_i)\in\Omega_3} S_{x_iy_i}$. So, we define the visibility function $w(x, y)$ at t as

$$w(x,y) = \exp(-\frac{d_{xy}}{R}) \cdot \exp(-\frac{\left|S^i_{xy}\right|}{\left|S^1_{xy}\right| + \left|S^2_{xy}\right|}) \tag{5}$$

where the first part represents the influence of visual ability of pedestrians on visibility function, d_{xy} represents the minimum distance between the cell (x, y) and cell (x_0, y_0) of exit, $d_{xy} = \min\limits_{(x_0,y_0)\in\Gamma_0} \sqrt{(x-x_0)^2 + (y-y_0)^2}$; the second part represents the influence of the surrounding pedestrians' moving direction on visibility function, if $S_{xy} > 0$, $i = 1$, or else $S_{xy} < 0$, $i = 2$.

According to the above analysis, compared to the cost potential field considering behavior fluctuation, the poor visual ability under emergency can also affect the cost of considering the comfort, which will lead to an increase in the cost of discomfort, so we extend the original cost of discomfort to three aspects: one is related to the density, one is caused by the behavior fluctuation, and the other is relevant to the visibility function. The cost function (2) is redefined as

$$\tau(x,y,t) = \frac{1}{v_{\max}} + a\rho^{\alpha} + b\eta^{\beta} + cw^{\gamma} \tag{6}$$

where ρ represents the local density in the pedestrian's visual field, and $\rho = \sum_{(x,y)\in D_{x,y}} n/\left|D_{x,y}\right|$, n represents the cell number in the visible area, $D_{x,y}$ represents the total number of cells in the visual area. Here, we choose the corresponding parameters as $\alpha = 2$, $\beta = 3$ and $\gamma = 1$. The weight parameters of local density, the behavior fluctuation and visibility cost are expressed by a, b and c, respectively, and $a + b + c = 1$ to meet the normalized condition.

2.4. Moving probability

In this paper, the Moore neighborhood is adopted and each occupied cell has eight neighboring cells, corresponding to nine probabilities for the pedestrian in the occupied cell to update his or her position (see Fig. 3). Assume (0, 0) is the coordinate of one walker, then the moving probability $p_{0,0}$ is specified as follows:

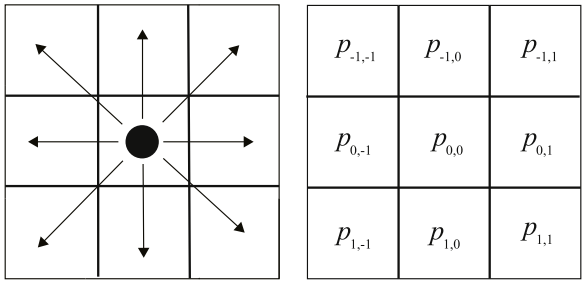

Fig. 3. (a) An occupied cell (0, 0) and its eight neighboring cells; (b) the corresponding probabilities for occupation in the next update step.

If $(0, -1)$ is empty, using the forward difference quotient, the difference quotient is $\phi'_{0,-1} = \left|(\phi^n_{0,-1} - \phi^n_{0,0})/d_{0,-1}\right|$; if $(0, 1)$ is empty, using the backward difference quotient, the difference quotient is $\phi'_{0,1} = \left|(\phi^n_{0,0} - \phi^n_{0,1})/d_{0,1}\right|$. Compute the difference quotient $\phi'_{x,y} = \left|(\phi^n_{0,0} - \phi^n_{x,y})/d_{x,y}\right|$ for $(x, y) \in \bar{S}_{xy}$, where $d_{x,y} = \sqrt{(x-0)^2 + (y-0)^2}$ is the distance between cell (x, y) and cell $(0, 0)$, $\phi^n_{x,y}$ is the potential field value of cell $(0, 0)$ in the nth step. Define the set

$$S_m = \{(x, y)\Big|\phi'_{0,0} = \min_{(x,y)\in\bar{S}_{x,y}}\phi'_{x,y}\} \tag{7}$$

and then define moving probability

$$p_{x,y} = \begin{cases} 0 & (x, y) \notin S_m \\ \dfrac{1}{|S_m|} & (x, y) \in S_m \\ 1 & (x, y) = (0, 0) \end{cases} \tag{8}$$

where $|S_m|$ is the number of elements in S_m.

2.5. Updating rules

In the initial state, due to the poor vision of pedestrians in the system, moving state of pedestrians can be divided into two parts according to the different regions:

(1) When pedestrians are located near the exit "region A" (see Fig. 1), the movement rules considering behavior fluctuation are adopted, i.e., the movement rules will vary according to the degree of tension. As $\mu \leq 0.05$, the behavior fluctuation caused by tension is approximately 0 and walkers being in a rational state will select the shortest route to the exit reasonably. Here, static field is introduced to describe the distance between each cell and the exit. It traverses the exit position region Γ of the static field value, and pedestrians will choose their moving paths based on the static field. It can be obtained according to the following function (9), i.e.,

$$S_{xy} = \max_{(x_1,y_1)\in\Omega}\left(\min_{(x_0,y_0)\in\Gamma}\sqrt{(x_1-x_0)^2+(y_1-y_0)^2}\right) - \min_{(x_0,y_0)\in\Gamma}\left(\sqrt{(x-x_0)^2+(y-y_0)^2}\right) \tag{9}$$

where $\min_{(x_0,y_0)\in\Gamma}\sqrt{(x_1-x_0)^2+(y_1-y_0)^2}$ represents the minimum distance between the neighbor cell (x_1, y_1) and cell (x_0, y_0) of exit when traversing all the cells in the exit position region Γ; $\max_{(x_1,y_1)\in\Omega}(\min_{(x_0,y_0)\in\Gamma}\sqrt{(x_1-x_0)^2+(y_1-y_0)^2})$ represents the maximum distance between the cell (x_1, y_1) and cell (x_0, y_0) of exit when traversing all the cells in the system Ω; $\min_{(x_0,y_0)\in\Gamma}(\sqrt{(x-x_0)^2+(y-y_0)^2})$ represents the minimum distance between the cell (x, y) and cell (x_0, y_0) of exit; Ω and Γ denote the system set and exit set, respectively. Assuming that each cell is empty or occupied and each pedestrian walks in a cell length in a time step or is static. During the movement, Moore neighborhood is adopted and the moving speed towards forward, left and right is $v = 1$ m/s. As $0.05 < \mu \leq 0.6$, the tension degree will lead to a linear increase of the behavior fluctuation. In this case, some pedestrians will have priority over others, the movement probability towards the diagonal direction of the cell will increase and the moving speed along the diagonal direction also increases to $v = 1.5$ m/s. As $\mu > 0.6$, namely, the tension degree exceeds the critical value of psychological endurance, the behavior fluctuation will have an exponential growth with the tension degree, as a consequence, pedestrians are completely controlled by panic and such unreasonable behaviors as impulse, beyond others and walking backward appear. The possible moving directions increase and the moving speed towards to each direction is same to that as $0.05 < \mu \leq 0.6$.

(2) When pedestrians are located in the poor vision area "region B" (see Fig. 1), the first choice for the blind pedestrians is to find a place where he/she feels safe. For example, to move along the wall, or to follow other pedestrians blindly in

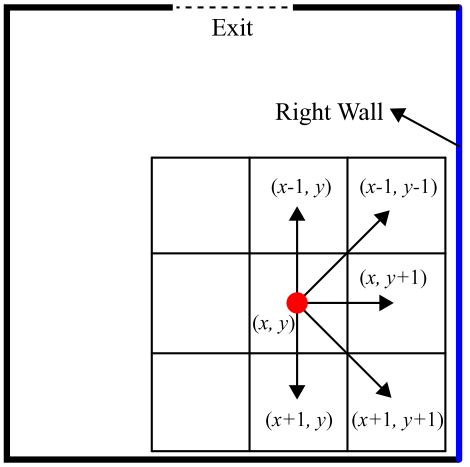

Fig. 4. The moving direction of the pedestrian near the right wall.

the visual range. Therefore, according to the pedestrians' visual range, we can divide into two cases: wall-visible area or wall-invisible area.

Case 1: wall-visible area. Here, take those pedestrians near the right wall as illustrated in Fig. 4 as example. As $\mu \leq 0.05$, pedestrians walk along the right wall. As $0.05 < \mu \leq 0.6$, the pedestrian will adjust selection strategy near the right wall and strive to be superior to other pedestrians in the wall position, and thus they can move towards $(x, y) \rightarrow (x-1, y)$, $(x, y) \rightarrow (x+1, y)$, $(x, y) \rightarrow (x, y+1)$. As $\mu > 0.6$, the exceeding nervousness will make pedestrians scramble for the target cell to reach the wall as quickly as possible, and there are five alternative directions to select. From the above analysis, if the distance to the wall is less than R, according to the psychology of pedestrians, the first choice is to move towards the wall, reach near the wall area, and then move along the wall. In this area, the corresponding moving speed is same to that near the exit region A.

Case 2: wall-invisible area. In such a situation, the distance to the wall is greater than R, with the consideration of pedestrian movements around, pedestrians will move according to formula (6). If $S_{xy} \neq 0$, the moving directions of the surrounding pedestrians are well concentrated and pedestrians will update their positions according to the rules of the potential function field (6), i.e., walkers will select the shortest route to the exit reasonably. If $S_{xy} = 0$, the moving directions of the surrounding pedestrian are more dispersed and walkers will move towards the empty cell in the Moore neighborhood randomly. In this area, the corresponding moving speed is also same to that near the exit region A.

3. Simulation results and discussions

Initially, all pedestrians are distributed randomly at the sites on the square lattice with the density $\rho = N/(L \times L)$. Following the above rules, all the cells' state are parallel updated. In the simulations, in order to remove the transient effect, the evacuation time was obtained by averaging over 20 runs. The related parameters are taken as $L = 100, W = 10, a = 0.2$, $b = 0.3, c = 0.5$ unless otherwise mentioned.

Firstly, we explore the macroscopic behavior characteristics under the poor vision. Fig. 5(a) and (b) give the typical spatial–temporal patterns during the evacuation process with $\mu = 0.1$ and $R = 10$ at initial density $\rho = 0.01$. According to the change of person location in the evolution map, Fig. 5(c) and (d) give the approximate moving path of the individual pedestrian in the system. Note that the polygonal path of pedestrians in the moving process is neglected. During the evacuation, the pedestrian will look for the wall as much as possible in poor visual environment. This process can be divided into two cases. One is that when pedestrians are looking for the walls, they first move to region A, then select the optimal path according to the static field value and move out of the system. The other is that the pedestrians find the location of the wall, but they could not judge their own optimal path, so there are two kinds of moving paths to select, i.e., Route 1 and Route 2, as shown in Fig. 5(d), in which Route 1 represents the optimal path to move along the wall. The simulation results describe pedestrian's moving characteristics at different locations under the poor vision environment and show that the larger possibility of blind movement will reduce the evacuation efficiency to a great extent, which is roughly in accordance with that in literature [33].

Next we study the influence of the visual radius on evacuation time. Fig. 6 gives the relationship between the evacuation time T and the total number N under different visual radius $R = 10, 30$. From Fig. 6, with the increase of time step, the pedestrian in the system decreases gradually until all pedestrians are removed out of the system. With the decrease of the total number of pedestrians in the system, the influence of visual ability on evacuation efficiency becomes more obvious. The curves have the similar tendency in Fig. 6. As $R = 10$, due to the poor visibility of the system, a small number of

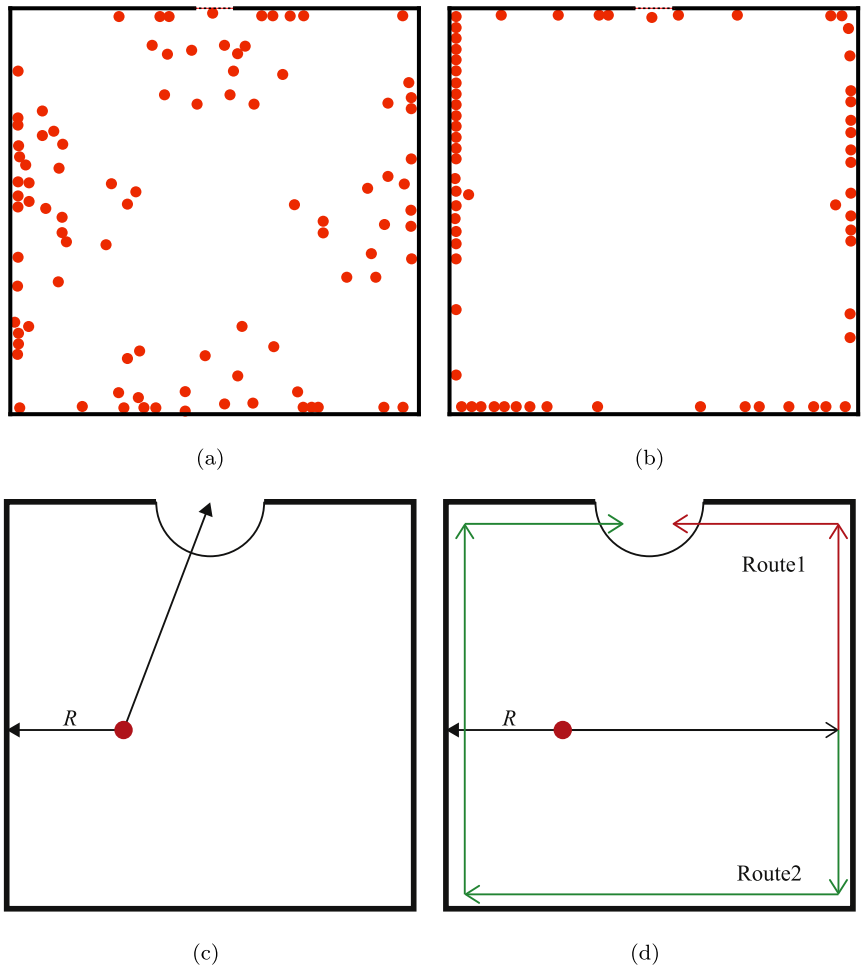

Fig. 5. The typical spatial–temporal patterns obtained at $\rho = 0.01, R = 10, \mu = 0.1$: (a) $t = 20$, (b) $t = 40$; (c)–(d) is the path map for a single pedestrian.

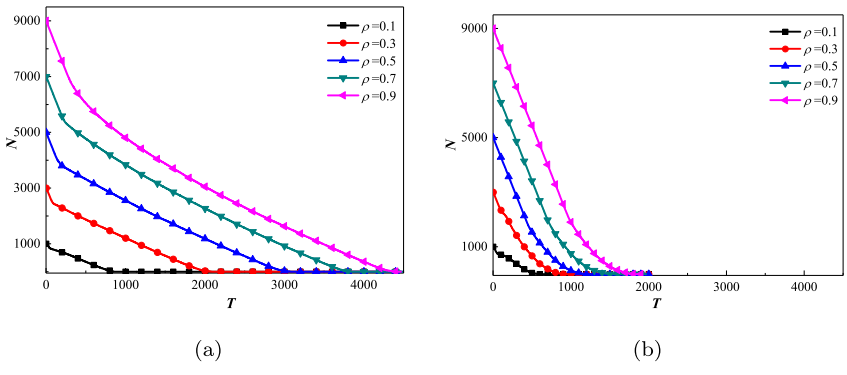

Fig. 6. The relationship between total number of pedestrian and evacuation time. (a) $R = 10$, (b) $R = 30$.

pedestrians arrive at the exit position in a short time, so the evacuation time drops obviously, but with the time evolution, most pedestrians choose the moving strategy along the wall because of the limitation of visual capacity radius, which makes the evacuation time decrease gradually (see Fig. 6(a)). As $R = 30$, under the same density, the evacuation time is far less than that of $R = 10$. The curve of the first stage is similar to the second stage. With the increase of visual radius, the perception to the surrounding environment becomes stronger, and the utilization of the exit position is also effectively improved, which

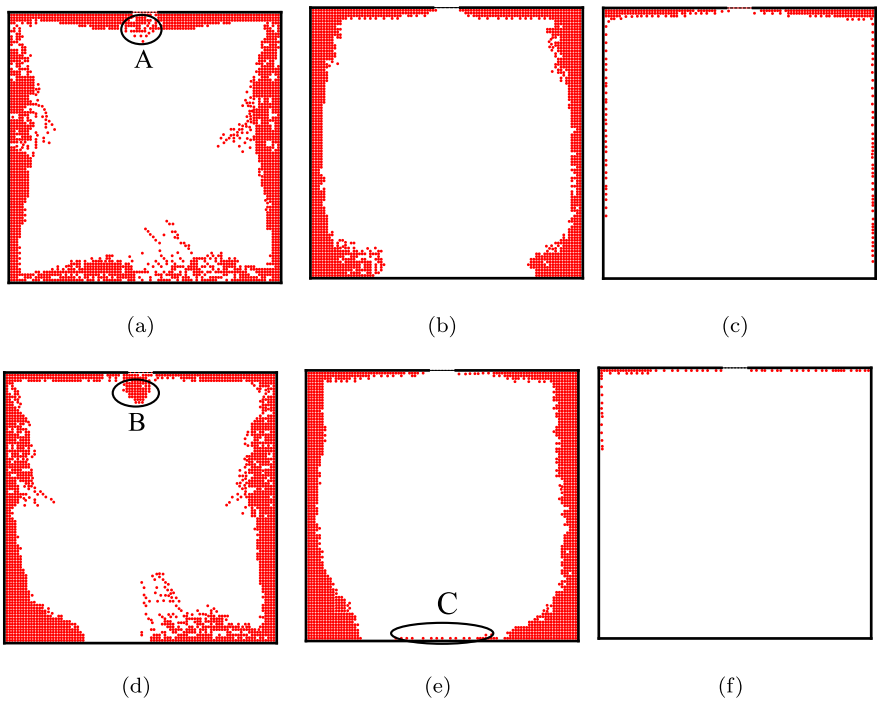

Fig. 7. The typical spatial–temporal patterns obtained at $R = 5$. $\mu = 0.3$: (a) $t = 40$, (b) $t = 110$, (c) $t = 1600$; $\mu = 0.7$: (d) $t = 40$, (e) $t = 110$, (f) $t = 1600$.

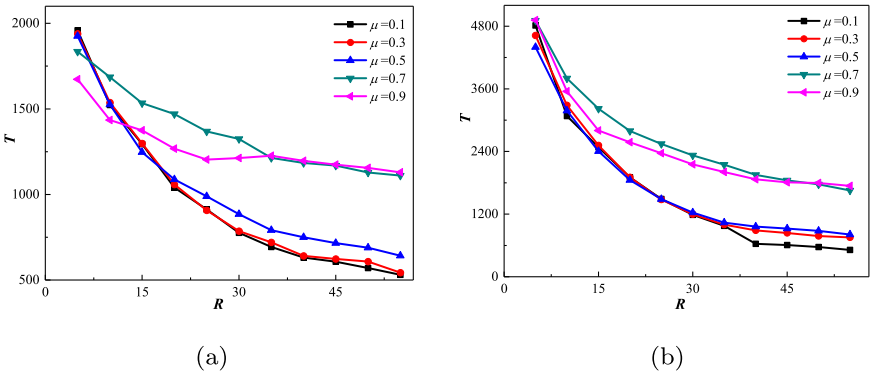

Fig. 8. The relationship between evacuation time T and different visibility radius R at $\mu = 0.1, 0.3, 0.5, 0.7, 0.9$. (a) $\rho = 0.2$, (b) $\rho = 0.5$.

will improve the evacuation efficiency of the system remarkably. Therefore, the size of the visible radius has a great influence on the evacuation efficiency.

Now, we explore the influence of different levels of tension on microscopic mechanism as $R = 5$, $\rho = 0.2$. Fig. 7 shows the snapshot of pedestrian flow at $\rho = 0.2$ under $\mu = 0.3$, $\mu = 0.7$, respectively. As time goes by, pedestrians in the system decrease gradually. Most pedestrians will choose along the wall strategy under the poor visibility environment. As seen in Fig. 7(a) and (d), at the initial stage, if the pedestrians are located in the exit area, the pedestrians will quickly assemble at the exit according to the optimal path strategy. With the time evolution, the evacuation capacity under $\mu = 0.3$ is higher than that $\mu = 0.7$. Due to the stronger interaction among pedestrians with $\mu = 0.7$, i.e., the collision, pushing, blindness caused by huge nervousness will hinder the evaluation process. A phenomenon that pedestrians move repeatedly around the lower wall can be observed from Fig. 7(e) (see region C). However, as $t = 1600$, with the decrease of total number of pedestrians, the evacuation efficiency of $\mu = 0.7$ is higher than that $\mu = 0.3$, which means that the sparse pedestrian distribution and the weak internal pressure among pedestrians makes the moving path become more flexible and moving speed become larger. As a result, the blindness caused by "irrational" state can effectively improve the efficiency of emergency evacuation.

Finally, we explore the influence of the visual radius on evacuation time under different level of tensions. Fig. 8 gives the relationship between the visual radius R and evacuation time T under different tension degrees $\mu = 0.1, 0.3, 0.5, 0.7, 0.9$.

From Fig. 8, it can be found that the evacuation time decreases with visual radius as a whole. However, with the consideration of tension degree and density, this variation is also different. At low density $\rho = 0.2$, the curves of $\mu = 0.7, 0.9$ have a small variation and have been less affected by visual ability. On the contrary, the curves $\mu = 0.1, 0.3, 0.5$ have a larger decline and have been affected by visual ability significantly. In addition, the increasing visual radius will make the evacuation time difference between $\mu = 0.1, 0.3, 0.5$ and $\mu = 0.7, 0.9$ become more obvious. The evacuation efficiency of $\mu = 0.1, 0.3, 0.5$ is higher than that $\mu = 0.7, 0.9$ at $R > 15$, but is lower at $R < 7$ (see Fig. 8(a)). This is because at low density and small visual radius, on the one hand, the collision and interaction among pedestrians can be ignored; on the other hand, the behavior variation caused by nervousness can also lead to the increase of pedestrian speed, which makes pedestrian leave the room quickly. However, with the increase of visual radius, compared with an exceeding nervousness, a moderate tension degree will improve the evacuation efficiency substantially (see Fig. 7(c) and (f)), which means that the coupling effect of moderate tension degree and visual radius has a positive role. At high density, the increasing tension degree will lead to an obvious reduction in evacuation efficiency with the increase of visual radius (see Fig. 8(b)). This is because at high density, the strong interaction, the more serious competition and congestion among pedestrians caused by the behavior fluctuation inevitably results in the reduction of the evacuation efficiency.

4. Conclusion

We develop an extended cost potential field cellular automata model to investigate the pedestrian evacuation under adverse sight conditions. The introduced visibility function describing poor vision can lead to the increasing cost of discomfort. The numerical simulations are performed to explore the effects of the visual radius, psychology tension, and pedestrian density on pedestrian evacuation dynamic properties. The typical spatiotemporal patterns under different level of tensions are explored. We have drawn the following important conclusions:

(1) In the poor visibility environment, most pedestrians will choose the moving strategy along the wall;
(2) In the process of emergency evacuation, the larger visual radius can improve evacuation efficiency to a certain extent. However, the continued increase of visual radius has little effect for the evacuation efficiency.
(3) Under different visual radius, the influence of psychology tension on the evacuation efficiency is also different. At low density, a moderate tension degree can improve the evacuation efficiency; however, at high density, the increasing tension will lead to an obvious reduction in evacuation efficiency.

These findings may provide a new insight into the pedestrian dynamic under an emergency. This will be helpful to control and guide pedestrian emotion reasonably. Although we have already obtained some important results, more consideration and investigations still need to be further done in future research.

Acknowledgments

This work was supported by the National Natural Science Foundation of China (Nos. 11762004 and 11747307), the Natural Science Foundation of Shanxi Province, China (201601D011013) and the Scientific Research Preferential Foundation of Shanxi Province for the Returned Overseas Chinese Scholars, China.

References

[1] D. Helbing, Traffic and related self-driven many-particle systems, Rev. Modern Phys. 73 (2001) 1067.
[2] D.C. Duives, W. Daamen, S.P. Hoogendoorn, State-of-the-art crowd motion simulation models, Transp. Res. C 37 (2013) 193–209.
[3] R.L. Hughes, A continuum theory for the flow of pedestrians, Transp. Res. B 36 (2002) 507–535.
[4] S.P. Hoogendoorn, P.H. Bovy, Pedestrian route-choice and activity scheduling theory and models, Transp. Res. B 38 (2004) 169–190.
[5] Y. Xia, S. Wong, C.W. Shu, Dynamic continuum pedestrian flow model with memory effect, Phys. Rev. E 79 (2009) 066113.
[6] Y.Q. Jiang, W. Zhang, S.G. Zhou, Comparison study of the reactive and predictive dynamic models for pedestrian flow, Physica A 441 (2016) 51–61.
[7] H.X. Ge, S.M. Lo, R.J. Cheng, A bidirectional pedestrian flow model with the effect of friction parameter, Internat. J. Modern Phys. C 25 (2014) 1450042.
[8] R.J. Cheng, H.X. Ge, J.f. Wang, An extended continuum model accounting for the driver's timid and aggressive attributions, Phys. Lett. A 381 (2017) 1302–1312.
[9] D. Helbing, P. Molnar, Social force model for pedestrian dynamics, Phys. Rev. E 51 (1995) 4282.
[10] D. Helbing, I. Farkas, T. Vicsek, Simulating dynamical features of escape panic, Nature 407 (2000) 487.
[11] T. Kretz, On oscillations in the social force model, Physica A 438 (2015) 272–285.
[12] Y. Ma, E.W.M. Lee, M. Shi, Dual effects of guide-based guidance on pedestrian evacuation, Phys. Lett. A 381 (2017) 1837–1844.
[13] H. Zhang, H. Liu, X. Qin, B. Liu, Modified two-layer social force model for emergency earthquake evacuation, Physica A 492 (2018) 1107–1119.
[14] M. Muramatsu, T. Irie, T. Nagatani, Jamming transition in pedestrian counter flow, Physica A 267 (1999) 487–498.
[15] Y. Tajima, T. Nagatani, Scaling behavior of crowd flow outside a hall, Physica A 292 (2001) 545–554.
[16] D. Helbing, M. Isobe, T. Nagatani, K. Takimoto, Lattice gas simulation of experimentally studied evacuation dynamics, Phys. Rev. E 67 (2003) 067101.
[17] H. Kuang, X. Li, T. Song, S. Dai, Analysis of pedestrian dynamics in counter flow via an extended lattice gas model, Phys. Rev. E 78 (2008) 066117.
[18] Q.Y. Hao, R. Jiang, M.B. Hu, B. Jia, Q.S. Wu, Pedestrian flow dynamics in a lattice gas model coupled with an evolutionary game, Phys. Rev. E 84 (2011) 036107.
[19] Y. Li, H. Jia, Y.N. Zhou, L. Yang, Simulation research on pedestrian counter flow subconscious behavior, Internat. J. Modern Phys. C 28 (2017) 1750025.
[20] C. Burstedde, K. Klauck, A. Schadschneider, J. Zittartz, Simulation of pedestrian dynamics using a two-dimensional cellular automaton, Physica A 295 (2001) 507–525.

[21] A. Kirchner, A. Schadschneider, Simulation of evacuation processes using a bionics-inspired cellular automaton model for pedestrian dynamics, Physica A 312 (2002) 260–276.
[22] J. Ma, W.G. Song, J. Zhang, S.M. Lo, G.X. Liao, k-Nearest-Neighbor interaction induced self-organized pedestrian counter flow, Physica A 389 (2010) 2101–2117.
[23] T. Ezaki, D. Yanagisawa, K. Nishinari, Pedestrian flow through multiple bottlenecks, Phys. Rev. E 86 (2012) 026118.
[24] R.Y. Guo, New insights into discretization effects in cellular automata models for pedestrian evacuation, Physica A 400 (2014) 1–11.
[25] L. Chen, T.Q. Tang, H.J. Huang, J.J. Wu, Z. Song, Modeling pedestrian flow accounting for collision avoidance during evacuation, Simul. Model. Pract. Theory 82 (2018) 1–11.
[26] L. Luo, Z. Fu, H. Cheng, L. Yang, Update schemes of multi-velocity floor field cellular automaton for pedestrian dynamics, Physica A 491 (2018) 946–963.
[27] J. Guan, K. Wang, F. Chen, A cellular automaton model for evacuation flow using game theory, Physica A 461 (2016) 655–661.
[28] L.A. Pereira, D. Burgarelli, L. Duczmal, F. Cruz, Emergency evacuation models based on cellular automata with route changes and group fields, Physica A 473 (2017) 97–110.
[29] T.Q. Tang, L. Chen, R.Y. Guo, H.Y. Shang, An evacuation model accounting for elementary students' individual properties, Physica A 440 (2015) 49–56.
[30] T.Q. Tang, Y.X. Shao, L. Chen, Modeling pedestrian movement at the hall of high-speed railway station during the check-in process, Physica A 467 (2017) 157–166.
[31] T.Q. Tang, S.P. Yang, H. Ou, L. Chen, H.J. Huang, An aircraft boarding model accounting for group behavior, J. Air Transp. Manag. 69 (2018) 182–189.
[32] G. Mantovani, L. Gamberini, M. Martinelli, D. Varotto, Exploring the suitability of virtual environments for safety training: signals, norms and ambiguity in a simulated emergency escape, Cogn. Technol. Work 3 (2001) 33–41.
[33] R. Nagai, T. Nagatani, M. Isobe, T. Adachi, Effect of exit configuration on evacuation of a room without visibility, Physica A 343 (2004) 712–724.
[34] T. Nagatani, R. Nagai, Statistical characteristics of evacuation without visibility in random walk model, Physica A 341 (2004) 638–648.
[35] W. Yuan, K.H. Tan, A model for simulation of crowd behaviour in the evacuation from a smoke-filled compartment, Physica A 390 (2011) 4210–4218.
[36] E.N. Cirillo, A. Muntean, Dynamics of pedestrians in regions with no visibilitya lattice model without exclusion, Physica A 392 (2013) 3578–3588.
[37] G.A. Frank, C.O. Dorso, Evacuation under limited visibility, Internat. J. Modern Phys. C 26 (2015) 1550005.
[38] X. Bing, H. Zhen, Z. Zong, Study on occupant evacuation model considering influence of direction sign, China Saf. Sci. J. 12 (2011) 27–33.
[39] S. Cao, W. Song, W. Lv, Z. Fang, A multi-grid model for pedestrian evacuation in a room without visibility, Physica A 436 (2015) 45–61.
[40] P. Zhang, X.X. Jian, S. Wong, K. Choi, Potential field cellular automata model for pedestrian flow, Phys. Rev. E 85 (2012) 021119.
[41] X.X. Jian, S. Wong, P. Zhang, K. Choi, H. Li, X. Zhang, Perceived cost potential field cellular automata model with an aggregated force field for pedestrian dynamics, Transp. Res. C 42 (2014) 200–210.
[42] F. Guo, X. Li, H. Kuang, Y. Bai, H. Zhou, An extended cost potential field cellular automata model considering behavior variation of pedestrian flow, Physica A 462 (2016) 630–640.
[43] X. Li, F. Guo, H. Kuang, H. Zhou, Effect of psychological tension on pedestrian counter flow via an extended cost potential field cellular automaton model, Physica A 487 (2017) 47–57.